

IL NUOVO CIMENTO  
DOI 10.1393/ncc/i2010-10527-y

VOL. 32 C, N. 5-6

Settembre-Dicembre 2009

COLLOQUIA: LaThuile09

## Status and perspectives of the $\mu^+ \rightarrow e^+\gamma$ decay search with the MEG experiment

M. GRASSI on behalf of the MEG COLLABORATION

*INFN, Sezione di Pisa - Largo Bruno Pontecorvo 3, 56127 Pisa, Italy*

(ricevuto il 10 Novembre 2009; pubblicato online il 15 Gennaio 2010)

**Summary.** — The MEG experiment aims at evidence of new physics beyond the Standard Model by searching for charged lepton flavour violation with the  $\mu^+ \rightarrow e^+\gamma$  decay. This experiment will improve the present experimental limit by two orders of magnitude in the upcoming three years. Novel detectors were developed for this measurement as well as multiple and redundant calibration methods which are mandatory to constantly monitor the performances of the apparatus. The status of the MEG experiment is reviewed and the future perspectives are discussed.

PACS 11.30.Hv – Flavor symmetries.

PACS 13.35.Bv – Decays of muons.

PACS 14.60.Ef – Muons.

### 1. – Introduction

The  $\mu^+ \rightarrow e^+\gamma$  decay is forbidden in the Standard Model of electroweak interactions because of the assumed symmetry of lepton flavour conservation. Though it has never been observed, with a current upper limit on the branching ratio of  $1.2 \times 10^{-11}$  set by the MEGA experiment [1], it is believed to take place at a certain level in any viable extension of the Standard Model [2, 3]. There is a wide class of models, namely Grand-Unified Supersymmetric theories, which predict  $\mu^+ \rightarrow e^+\gamma$  decay to exist with a branching ratio in the range  $10^{-14}$ – $10^{-11}$ .

The MEG experiment will search for this lepton flavour violating decay with a sensitivity of  $\approx 10^{-13}$  on the branching ratio. The discovery of this decay would be the first direct evidence of new physics beyond the Standard Model, while the absence of the signal in this range would pose important constraints for the development of new theories.

### 2. – Signal and background

The  $\mu^+ \rightarrow e^+\gamma$  decay is characterized by a two-body final state, with the positron and photon being coincident in time and emitted back-to-back in the rest frame of the muon, each with an energy equal to half that of the muon mass.

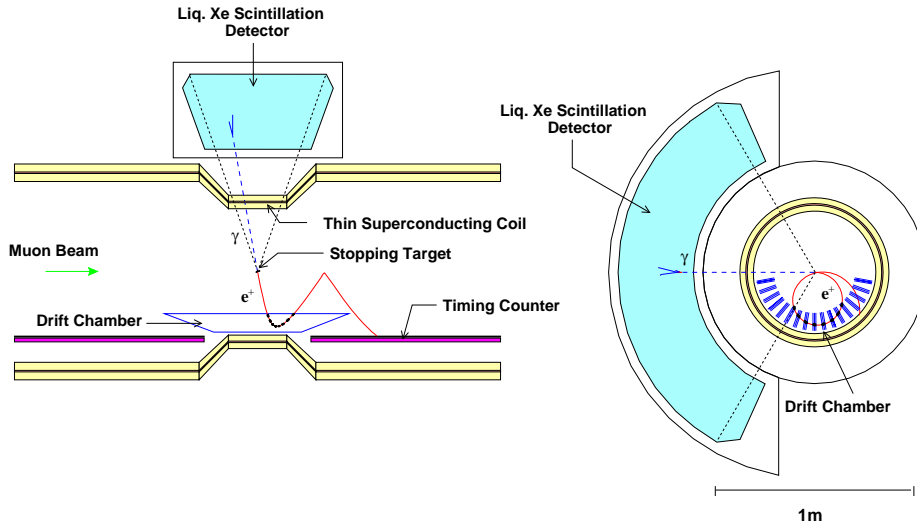


Fig. 1. – Schematic drawing of the MEG detector.

The two major sources of background are the radiative muon decay (RMD)  $\mu^+ \rightarrow e^+ \nu_e \bar{\nu}_\mu \gamma$  and the accidental coincidences between a high-energy positron from the normal muon decay  $\mu^+ \rightarrow e^+ \nu_e \bar{\nu}_\mu$  (Michel decay) and a high-energy photon from sources such as RMD, positron annihilation-in-flight or bremsstrahlung. Both types of background can mimic a signal event by having an almost back-to-back photon and positron. It can be shown [4], taking into account the muon rate as well as the acceptances and resolutions, that the accidental contribution, which scales quadratically with the muon rate, dominates.

Hence the keys to suppress such backgrounds lie in having a continuous muon beam, a good-quality beam transport system and precision detectors with excellent spatial, temporal and energy resolutions. The design of the MEG experiment has been inspired by these arguments.

### 3. – The detector

A schematic view of the detector is shown in fig. 1.

The MEG experiment [5] is operated at the Paul Scherrer Institut (PSI) in Switzerland, on the  $\pi E5$  beam line. The positive muon beam of 28 MeV/c momentum, with intensity up to  $10^8 \mu/s$  in a  $\sim 0.5$  cm radius spot, is brought to stop in a thin partially depolarizing polyethylene target after passing a stage in which most of the contaminating positrons are eliminated.

Positrons originating from muon decay are analyzed in the COBRA (COntant-Bending-RAdius) spectrometer consisting of a superconducting magnet with a gradient magnetic field, a tracking system of low-mass drift chambers and two fast-scintillator timing-counter arrays.

The gradient magnetic field in the spectrometer, ranging from 1.27 Tesla at the centre to 0.49 Tesla at either end, is shaped so that monochromatic  $e^+$ s from the target follow trajectories with an almost constant projected bending radius, independent of their emission angle over a wide angular range. Furthermore the sweeping capability of

the non-uniform magnetic field reduces the persistence of low longitudinal momentum  $e^+$ s in the tracking volume. Both features greatly reduce the accidental pile-up of the Michel positrons, decrease the pattern recognition complexity and enhance the system efficiency.

The drift chamber system (DCH) consists of 16 radially aligned modules, spaced at  $10.5^\circ$  intervals and placed at equal distance from the target. Each drift chamber module contains two staggered layers of anode wire planes each of nine drift cells. The two layers are separated and also enclosed by  $12.5 \mu\text{m}$  thick cathode foils with a Vernier pattern structure. The chambers are operated with a helium:ethane (50:50) gas mixture. The DCH system thickness along the positron trajectory is only  $2.0 \times 10^{-3} X_0$  and the design momentum resolution for signal  $e^+$ s results in  $0.4 \text{ MeV}/c$  FWHM.

Positron timing information originates from two scintillator timing-counter arrays (TC), placed at each end of the spectrometer. Each array consists of 15 BC404 plastic scintillator bars, with 128 orthogonally placed BCF-20 scintillating fibres. Each bar is read out at both ends by fine-mesh photomultiplier tubes, while the fibres are viewed by avalanche photo-diodes. The  $e^+$  emission time is measured with resolution of  $0.1 \text{ ns}$  FWHM, while the impact point on the TCs, given by the fibers, provides directional information on the positron for triggering purposes.

The photon detector is a 900 litre homogeneous volume of liquid xenon (LXe) that subtends a solid-angle acceptance of  $\sim 10\%$ . It uses scintillation light to measure the total energy released by the  $\gamma$ -ray as well as the position and time of its first interaction. In total, 846 photomultiplier tubes (PMTs), internally mounted on all surfaces and submerged in the xenon, are used. The advantages of using liquid xenon are the fast response, the large light yield and the short radiation length. Stringent control of contaminants is necessary since the vacuum ultra-violet (VUV) scintillation light is easily absorbed by water and oxygen even at sub-ppm levels. The xenon is therefore circulated in liquid phase through a series of purification cartridges, and in gas phase through a heated getter. The expected energy, timing and position resolutions on signal photons are, respectively,  $4.5\%$ ,  $0.1 \text{ ns}$  and  $5 \text{ mm}$ , expressed in FWHM.

The electronics signals generated by LXe and TC photomultipliers are actively split and go to both the trigger and the waveform digitizer systems, while DCH signals are directly sent to the latter.

The waveform digitizers are based on the multi-GHz Domino Ring Sampler chip (DRS [6]), which can sample ten analog input channels into 1024 sampling cells each at speeds of up to  $4.5 \text{ GHz}$ . The sampling speed for the drift chamber signals is  $500 \text{ MHz}$ , while that of the PMT signals from the photon detector and timing counters is  $1.6 \text{ GHz}$ . This strategy gives maximum flexibility, allowing various read-out schemes, such as zero suppression, on an event-by-event basis for various trigger types. The system achieves an excellent pile-up recognition, together with superior timing and amplitude resolutions, compared to conventional schemes.

The trigger is based on fast information from the two detectors using PMTs: the liquid-xenon photon detector and the positron timing counters. It makes use of a subset of the kinematic observables from  $\mu$ -decay at rest, requiring an energy deposit in the photon detector in an interval containing  $52.8 \text{ MeV}$ , a time coincident positron hit on the timing counters and a rough collinearity of the two particles, through a look-up table. The decay kinematics is reconstructed by electronics boards arranged in a triple layer tree-structure. The signal digitization is executed by means of a  $100 \text{ MHz}$ , 10-bit flash analog-to-digital converters. A pre-scaled, multi-trigger event scheme is used for data-taking allowing calibration, background and signal events to be read-out together. The

typical event signal rate was 5 Hz, and the total DAQ rate was 6.5 Hz, with an average livetime of  $\sim 84\%$ .

The trigger and the digitizers systems are contained in nine VME crates, individually read out by front-end computers. The nine event fragments are sent over a Gigabit Ethernet link to a central event building computer that provides data storage.

#### 4. – The run 2008

We operated the apparatus for the  $\mu^+ \rightarrow e^+\gamma$  search from September to December 2008. In this period  $\sim 10^{14}$  muons were stop in the target at a stop rate of  $3 \times 10^7 \mu/s$ .

During the data-taking period the light yield of the photon detector was continuously increasing due to the purification of the liquid xenon being performed in parallel with the event acquisition. The absolute Xenon light yield increased by  $\sim 45\%$ . Furthermore, an increasing number of drift chambers were affected by frequent high-voltage trips. Over the data-taking period this caused a reduction of the positron detection efficiency by a factor of three.

The increase of xenon light yield was carefully monitored with the various calibration tools, described in the next section, and it is taken into account in the determination of the energy scale. The trigger thresholds were also accordingly adjusted to guarantee an uniform efficiency and a constant acquisition rate.

The drift chamber efficiency drop reduced the experiment sensitivity to the signal. We are developing a normalization scheme which depends only on the ratio of the signal positron efficiency over that of the normal muon decay positron. This scheme is therefore independent of a difficult determination of the absolute DCH efficiency.

#### 5. – Monitoring and calibrations

The number of background events entering the signal region can vary in case of time dependence of the detector efficiencies or resolutions. It is therefore necessary to have a continuous and reliable monitoring system of all the experimental resolutions involved in the determination of the signal region.

During the normal data taking, on a daily basis, light from variable intensity LEDs was used to measure the LXe PMT gain, while  $\alpha$  events of 5.5 MeV from point like sources deposited on thin wires [7] were used to measure the PMT quantum efficiencies and the liquid xenon optical properties.

Three times per week the muon stopping target was removed, an extendable beam pipe places a  $\text{Li}_2\text{B}_4\text{O}_7$  target at the centre of the detector and protons were shut on the target by a dedicated CW-accelerator placed downstream of the experiment. Photons of  $E_\gamma = 17.67$  MeV from  ${}^7\text{Li}(p, \gamma){}^8\text{Be}$  allowed the monitoring of the LXe detector energy scale, while coincident  $\gamma$ 's of  $E_\gamma = 4.4, 11.6$  MeV from  ${}^{11}\text{B}(p, \gamma){}^{12}\text{C}$ , detected simultaneously by the TC and the LXe, allow the determination of time offsets.

Once a week an entire day of radiative muon decay (RMD) acquisition at reduced beam intensity was performed, with the trigger requirements relaxed to include non back-to-back positron-photon events in a wider energy range.

Two runs of pion charge-exchange reaction ( $\pi^- p \rightarrow \pi^0 n \rightarrow \gamma\gamma n$ ) were conducted, one at the beginning and one at the end of the data acquisition period. Pion capture at rest on hydrogen produces photons with energy  $54.9 < E_\gamma < 83.0$  MeV. By detecting one of these photons with the LXe detector and the other at  $180^\circ$  by means of a set of NaI crystals, two mono-energetic calibration lines at the extremes of the energy spectrum are

obtained. These enable measurement of the energy scale and uniformity. Dalitz decays ( $\pi^0 \rightarrow \gamma e^+ e^-$ ) were also collected by using a photon-positron coincidence trigger, and used to study the detector time synchronization and resolution.

The combined use of all these methods enables the investigation of possible systematic variations of the apparatus.

## 6. – Analysis procedure and radiative muon decay signal

The number of signal events will be determined by means of a maximum-likelihood fit of the physical observables:  $E_\gamma$ ,  $E_{e^+}$ ,  $\Delta t_{\gamma e^+}$  and  $\Delta\Theta_{\gamma e^+}$ . In order to prevent any bias in the definition of the probability density functions (PDF) the events falling in a observable window around the signal region, often called “blinding-box”, are written to a separate and protected data stream. The analysis parameters and the background are optimized on the events outside the “blinding-box”.

The RMD events are the second background source of the experiment. The precise estimation of the PDFs for these events is of great importance because the kinematical observables are correlated. Special runs at reduced  $\mu$ -stop rate were taken to clearly identify the RMD signal in a wide observables region, well extended beyond the “blinding-box”. The small number of collected RMD events,  $\sim 400$ , evaluated with the detector efficiencies and acceptance, is in agreement within 20% the published measurement [8].

## 7. – Expected final sensitivity and perspectives

The accidental background, which turns out to be the dominant component, contributes with  $\approx 3 \times 10^{-14}$  events per muon decay, for the running muon stop rate of  $R_\mu = 3 \times 10^7 \mu/s$ .

With this  $R_\mu$  stop rate, the design detector resolutions and a total running time of  $\sim 3 \times 10^7$ s, the single event sensitivity (SES) of MEG results  $\sim 5 \times 10^{-14}$ . The sensitivity can be converted into 90% confidence level upper limit of  $\sim 1.2 \times 10^{-13}$ , in case of no signal observed.

As already mentioned, we are progressing in the comprehension of the detector systematics and we are exploiting the large amount of calibration data to improve the reconstruction algorithms. The MEG Collaboration is planning to complete the analysis of the data taken in the first three months of detector running by summer 2009.

The light yield of the liquid-xenon detector was constantly increasing and, during the winter 2009 shutdown, the xenon was completely evaporated and purified. The light yield is therefore expected to be totally recovered for the next running period. The drift chamber detector were disassembled and a weak point on a printed circuit board, possible cause of the high-voltage trips, was identified and fixed. The run 2009, with improved detectors, is scheduled to start in August for a running period equivalent to the one of 2008.

## REFERENCES

- [1] BROOKS M. L. *et al.*, *Phys. Rev. Lett.*, **83** (1999) 1521.
- [2] BARBIERI R. *et al.*, *Nucl. Phys. B*, **445** (1995) 215.
- [3] HISANO J. *et al.*, *Phys. Rev. B*, **391** (1997) 341.
- [4] KUNO Y. and OKADA Y., *Rev. Mod. Phys.*, **73** (2001) 151.

- [5] BALDINI A., MORI T. *et al.*, *The MEG experiment: search for the  $\mu \rightarrow e\gamma$  decay at PSI*, available at <http://meg.psi.ch/docs>.
- [6] RITT S., *Nucl. Instrum. Methods A*, **518** (2004) 470.
- [7] BALDINI A. *et al.*, *Nucl. Instrum. Methods A*, **565** (2006) 589.
- [8] CRITTENDEN R. R. *et al.*, *Phys. Rev.*, **121** (1961) 1823.